ANNUAL REVIEWS

Annual Review of Analytical Chemistry

Wearable Microfluidics for Continuous Assay

Pei-Heng Lin,[1,2,*] Hsin-Hua Nien,[1,3,4,5,*] and Bor-Ran Li[1,2,6]

[1]Institute of Biomedical Engineering, National Yang Ming Chiao Tung University, Hsinchu, Taiwan; email: liborran@nytu.edu.tw

[2]Department of Electronics and Electrical Engineering, National Yang Ming Chiao Tung University, Hsinchu, Taiwan

[3]College of Electrical and Computer Engineering, National Yang Ming Chiao Tung University, Hsinchu, Taiwan

[4]Department of Radiation Oncology, Cathay General Hospital, Taipei, Taiwan

[5]School of Medicine, College of Medicine, Fu Jen Catholic University, New Taipei City, Taiwan

[6]Center for Emergent Functional Matter of Science, National Yang Ming Chiao Tung University, Hsinchu, Taiwan

Annu. Rev. Anal. Chem. 2023. 16:181–203

First published as a Review in Advance on March 8, 2023

The *Annual Review of Analytical Chemistry* is online at anchem.annualreviews.org

https://doi.org/10.1146/annurev-anchem-091322-082930

*These authors contributed equally to this article

Keywords

lab-on-chip devices, wearable device, microfluidic analysis, microfluidic design, biomarker sensing

Abstract

The development of wearable devices provides approaches for the realization of self-health care. Easily carried wearable devices allow individual health monitoring at any place whenever necessary. There are various interesting monitoring targets, including body motion, organ pressure, and biomarkers. An efficient use of space in one small device is a promising resolution to increase the functions of wearable devices. Through integration of a microfluidic system into wearable devices, embedding complicated structures in one design becomes possible and can enable multifunction analyses within a limited device volume. This article reviews the reported microfluidic wearable devices, introduces applications to different biofluids, discusses characteristics of the design strategies and sensing principles, and highlights the attractive configurations of each device. This review seeks to provide a detailed summary of recent advanced microfluidic wearable devices. The overview of advanced key components is the basis for the development of future microfluidic wearable devices.

1. INTRODUCTION

Wearable devices are an innovative solution for health care problems (1–5). Technological advancement has brought new opportunities to overcome the limitations of centralized health care systems. Individuals that begin monitoring health conditions obtain prioritized diagnosis and treatment from doctors by giving them dynamic insights into their personal physiological conditions. Wearable devices record long-term human physical activities and physiological and biochemical parameter variance in daily life (6). The development of the devices is in the form of accessories, including wristbands, armbands, glasses, and patches or tattoos, or as a continuous body attachment probe for physiological indicators (7). These platforms are designed to be comfortable for the real-time continuous monitoring of human physiological information through biofluids (8). Both physical and chemical sensors would be advantageous for individuals to monitor health and illness states and benefit many types of users, including athletes, patients, and elderly individuals (9, 10).

In the field of health care, wearable devices are often portable medical electronic devices that measure, record, and analyze health information (11, 12). By intelligent integration with microelectronics and computing power, the series of dynamic data are combined with a large database, supporting various technology connections, classification, cloud services, and storage of personal information in a dynamic state. The sensor readouts generate a personalized baseline indicating health conditions and give a warning when a deviation is different from the near-normal state (13). The information is also stored in a health care database, and the variation among different groups sets up a fingerprint to approach a more precise and optimal diagnosis. With immediate indicators for patient signs and biomarkers, the results provide a wide range of guidance on diet, exercise, and administration of medicine for intelligent detection for disease prevention and long-term health care (14).

In traditional medical diagnosis, samples such as blood and urine are routinely used as the analytical targets of standard technologies for further physiological or metabolite detection in medical centers (15, 16). Even good conventional handheld sensing devices, such as blood analyzers, glucose meters, and lactate analyzers, rely on invasive methods for derived blood samples. The intrusive approaches of these devices cause pain and risk factors for patients and impede the continuous measurement of physiological signals. Currently, continuous monitoring systems, such as continuous glucose monitoring (CGM) systems (17, 18), have been recognized as features in automatically recording metabolite conditions. In the CGM system, sensors measure the blood glucose concentration through interstitial fluid (ISF) (**Figure 1**). The ISF glucose level is converted to blood glucose concentration through calibration for continuous measurements through the day and night. Although the sensors provide changeover readouts per hour, this type of sensor is still defined as minimally invasive and requires a small probe to be inserted or implanted under human skin (19, 20). Such implantable devices still face challenges in accessing noninvasive devices in medical applications.

The development of microfluidic systems applied in wearable devices facilitates the effective, noninvasive, continuous monitoring of physiological states in individuals (21). Microfluidics is multidisciplinary for precise regulation and manipulation in geometrically confined small-scale fluids (22). Microfluidics has practical applications, such as cell size sorting, particle formation, particle trapping, and gradient generation, and is widely applied in the fields of organs-on-chip, cell culture, drug delivery, biochemistry, and biotechnology (23–25). Microfluidics offers great opportunities for integration with wearable sensors that complete the sample-to-answer solution (26). This review provides a detailed summary of recent advanced microfluidic wearable devices. It introduces microfluidic wearable devices and their applications and discusses the characteristics of design strategies and sensing principles.

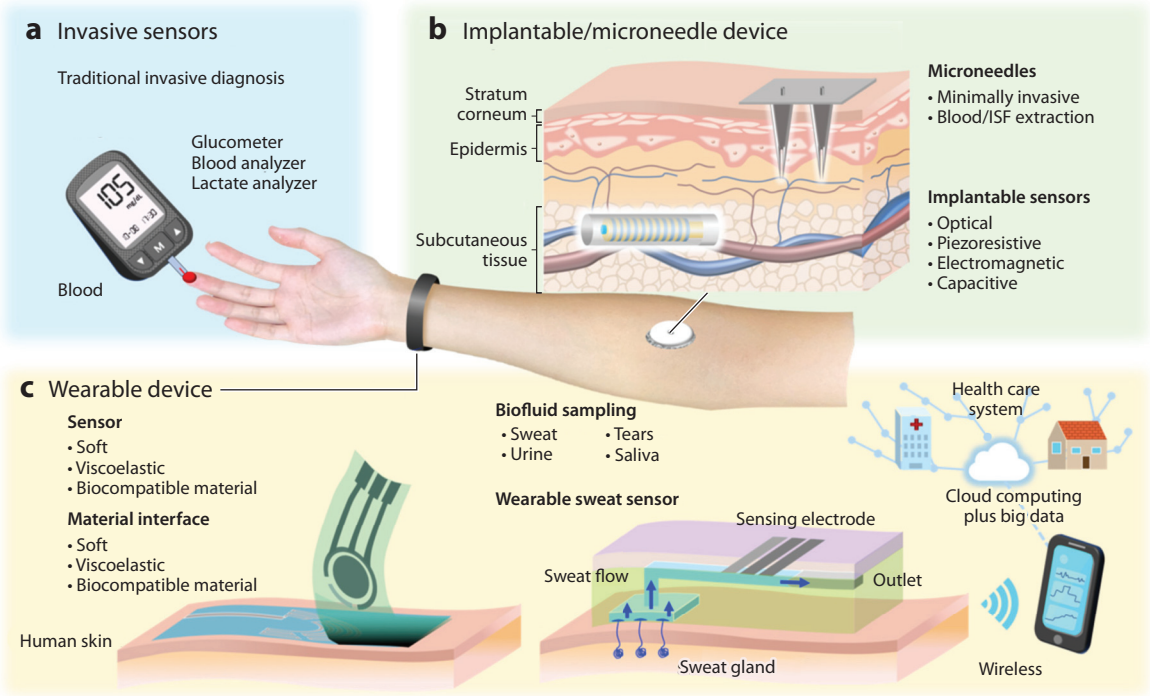

Figure 1

Schemes depicting the sensing system in personal health care. (*a*) Invasive sensors, (*b*) an implantable/microneedle device, and (*c*) a wearable device. Abbreviation: ISF, interstitial fluid.

2. BIOSENSING FOR DIFFERENT BIOFLUIDS

2.1. Interstitial Fluid

ISF is a valuable biofluid source for continuous measurement in wearable devices (27–29). This body fluid surrounds cells and fills the extracellular space between tissues, constituting the internal environment for the body and comprising 15–25% of its weight. ISF forms by extravasation of plasma through capillary exchange and is regulated through metabolic and other processes (30). The nutrients and side products in ISF provide systemic information that is generally a combination of serum and cellular compositions. Both the protein and metabolite levels in ISF under the skin have shown many similarities as biomarkers, but 50% of the protein in ISF is not found in plasma (31–33), suggesting that ISF might be a unique source of biomarkers. Because many studies have used ISF for the continuous detection of chronic disease, organ failure, and drug efficacy over the past decades (9), implantable devices can detect ISF variance directly under the skin. Isensee et al. (34) reported a quantum cascade laser-based optofluidic glucose sensor for use as a long-term continuous glucose measurement implant. A miniaturized optofluidic interface was used to measure the characteristic midinfrared absorption of glucose concentration within 5 min. The sensor remained stable while tracing changes during an extended 42-day in vitro test. It also evaluated the Parkes error grid analysis with an acceptable medical range of 100% in zone A. Despite the fact that implantable devices fulfill the requirements of fast response time, high stability, and long use life, implantation causes intractable problems owing to the risk of at-home self-administration complications such as local tissue injury and the unpredictable foreign body reaction.

The microneedle is categorized as minimally invasive and as an alternative tool that detects ISF in a nearly pain-free manner. The tip of the needle, sometimes with the microfluidic channel, penetrates through the stratum corneum without contacting nerves in the dermal regions and transports the biofluid back to the sensing system. Ranamukhaarachchi et al. (35) developed a therapeutic drug monitoring system by hollow microneedles that extract ISF in extremely small volumes, approximately 0.6 nL, for real-time drug concentration monitoring. The microneedle-optofluidic biosensor is functionalized and coated with gold on the surface, which attracts a specific drug molecule, vancomycin, in this case with 0.41 AU/decade sensitivity and rapid measurement time (<5 min). Another example of a microfluidic microneedle array is reported by Jina et al. (36). They presented a continuous microneedle-based glucose monitoring system. The tip of the hollow microneedle was placed in the epidermis without damaging blood vessels for ISF sampling for up to 72 h. The microfluidic channel-transported biofluid reached the glucose oxidase-fixed electrode that is able to measure the current change with the amperometric method. The minimally invasive glucose microneedle was able to measure glucose levels successfully, providing trends similar to a commercial blood glucometer. As a result, the Clarke error grid showed 74.6% of predicted values filled in zone A and 98.4% in zone A+B, with low-level systematic and random error (with a mean value of the absolute relative differences of 15%).

For noninvasive chemical sensing, most biosensors have employed reverse iontophoresis for a continuous approach in the real-time measurement of target biomarkers (37–39). Chen et al. (40) demonstrated a new prospect of simultaneous ISF sampling and analysis on a wearable epidermal platform for glucose detection. The system integrates an ultrathin skin-like biosensing system with a biocompatible battery. The subcutaneous sensor acts through hyaluronic acid for ISF extraction with the reverse iontophoresis at the anode and cathode electrodes. The performance of the ISF shows high glucose sensitivity (130.4 mA/mM) and high correlation (>0.9) compared with clinically measured blood glucose concentrations in in vivo human clinical trials (**Figure 2**).

2.2. Saliva

Saliva, an oral biofluid, is secreted from three major salivary glands of the basic secretory units, the clusters of acini. The components of saliva diffuse from blood, including water, electrolytes, cells, enzymes, hormones, metabolites, and antimicrobial agents, which are specific and informative biomarkers for disease diagnosis (41–43). Meanwhile, saliva detection could also be applied in food intake measurements for the variance of metabolites and personalized nutrition. Targeting saliva provides practical advantages in rapid collection, large analyte volume, continuous flow, and relatively clean samples for reliable measurements (44, 45). Arakawa et al. (46) demonstrated a mouthguard glucose sensor in the development of monitoring the glucose level in saliva (**Figure 2**). The saliva glucose sensor is based on enzymatic detection through an amperometric method. The mouthguard quantified the glucose concentration in the range of 1.75 to 10,000 μmol/L, which covered the glucose level of 20 to 200 μmol/L in saliva. Lee et al. (47) reported an ultrathin and soft electronic platform in the oral cavity with miniaturized sensors for the measurement of sodium intake with real-time monitoring through Bluetooth wireless telemetry. The microstructures of sodium potentiometric sensors are integrated into a chip-scale stretchable microporous elastomeric membrane. The in vivo sodium level changes from different foods, including vegetable juice, chicken noodle soup, and potato chips, demonstrate the potential for real-time quantification of sodium intake. Such continuous ion monitoring has the potential for preventing diet-related diseases and providing real-time feedback and physiological suggestions for nutritional advice. García-Carmona et al. (48) developed a wearable chemical sensor for infant saliva monitoring. The pacifier, integrated with wireless electronic electrochemical metabolite sensors, effectively pumps saliva and creates a unidirectional fluid flow to the sensing platform.

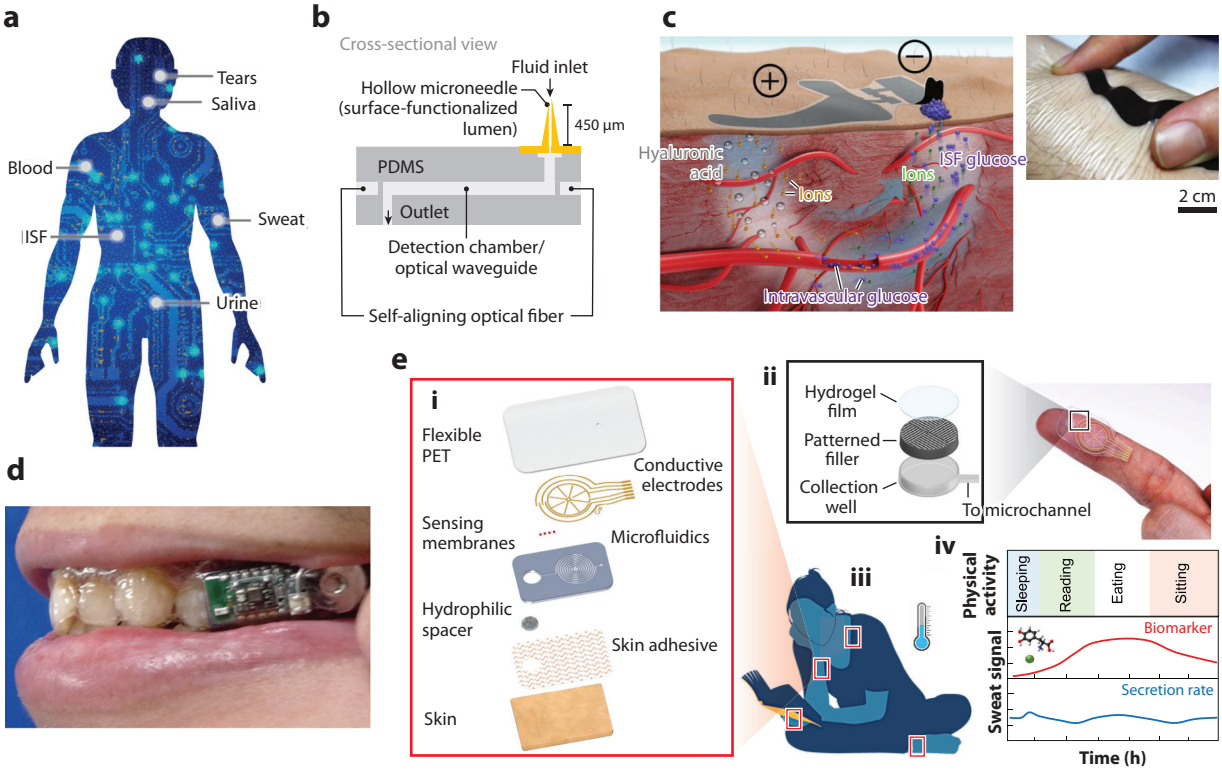

Figure 2

Wearable biosensors for health care monitoring of physiological biofluids. (*a*) Illustration of the applied physiological biofluid of wearable biosensors. (*b*) The integrated microneedle optofluidic biosensor for therapeutic drug monitoring. Panel adapted from Reference 35 (CC BY 4.0). (*c*) A noninvasive, ultrathin skin-like wearable sensor for ISF glucose monitoring. Panel adapted from Reference 40 (CC BY-NC 3.0). (*d*) A wearable mouthguard for the detection of ascorbic acid and uric acid in saliva with an interference rejection membrane. Panel adapted with permission from Reference 46; copyright 2020 American Chemical Society. (*e*) Wearable microfluidic patch for natural sweat collection that enables monitoring of the secretion rate at rest. (*e*, *i*) Components of each layer of the device. (*e*, *ii*) Laminated components of the hydrophilic filler assist rapid sweat uptake at low secretion rates. (*e*, *iii*) Dynamic sweat secretion can be monitored at various locations during daily activities. (*e*, *iv*) Sweat secretion rate and biomarker components can be monitored continuously without extra sweat stimulation during daily activities. Panel adapted from Reference 69 (CC BY 4.0). Abbreviations: ISF, interstitial fluid; PDMS, polydimethylsiloxane; PET, polyethylene terephthalate.

The wearable saliva platform was demonstrated for real-time amperometric glucose monitoring with a linear range of response (LRR) from 0.1 to 1.4 mM and a limit of detection of 0.04 mM. Most wearable devices based on saliva detection are in the form of mouthguards or fixed in the oral cavity for continuous measurement. Because such oral insertion devices require a certain volume, their bulkiness significantly causes discomfort and is impractical for long-term use.

2.3. Tears

Tear-based wearable devices have gained popularity in recent years due to the cleanliness of the sample and stability of the device. Tears are secreted by lacrimal glands as a protective layer for lubricating, removing irritants, and aiding the immune system. Tear biofluid contains relatively high levels of biomarkers that diffuse directly from blood, and the concentration is more closely correlated with blood compared to other biofluids (49).

To continuously monitor physiological conditions in real time through tears, contact lens–based wearable devices integrated with microfluidic systems provide a great approach to sampling challenges, including small sample volumes, rapid evaporation, and a lack of biofluid for users. Agaoglu et al. (50) reported wearable passive integrated microfluidic contact lenses for the measurement of intraocular pressure (IOP). The microfluidic strain sensor detected the volume expansion and compression with a reproducible volume change of a closed channel. The smart wearable sensor showed a detection limit of <0.004% for biaxial strain with the smartphone–macrolens combination imaging system. An et al. (51, 52) also developed continuous IOP monitoring contact lenses through a compression-sensing layer of micropatterning soft elastomer and a reference layer. The annular sensing chamber is filled with dyed solution as the IOP variance indicator. The deformation of the sensing layer under pressure can be optically observed by a smartphone. The sensitivity of the sensing pressure was 0.708 mm/mm Hg in the range of 0 to 40 mm Hg. Kim et al. (53) reported soft multifunctional contact lenses for the electrochemical detection of glucose in tears and IOP. The device integrated a graphene-Ag nanowire hybrid structure into soft contact lenses and successfully detected tear glucose and IOP with high transparency (>91%) and stretchability (~25%). Tear glucose was detected through a field-effect transistor-based glucose sensor ranging from 1 μM to 10 mM. The increase in IOP changes the radius of curvature of the cornea, which changes the relative position of the circuit and finally results in low frequency. The IOP detection ranged from 5 to 50 mm Hg with a linear slope of 2.64 MHz/mm Hg. Yang et al. (54) developed flexible, wearable, biocompatible methacrylated poly(dodecanediol citrate) polymer (mPDC)-based contact lenses that embedded chemical substrates and detected metabolites in tears by color change, including glucose, chloride, and urea. The concentration readouts were imaged by the mobile photography system with red-green-blue (RGB) analysis. Moreddu et al. (55, 56) developed microfluidic contact lenses for in situ metabolite sensing for pH, glucose, protein level, nitrite ions, uric acid level, and tear volume detection. The spiral lens provides an alternative way to measure tear fluid production and may reduce the discomfort of the dry eye Schirmer's test (56). The microchannel is inscribed in commercial contact lenses with a central pathway with four sensing branches for metabolite detection. Within 15 s of response time, the detection sensitivity showed 12.23 nm/pH unit, 1.4 nm/mmol L^{-1} of glucose, 0.49 nm/g L^{-1} of proteins, and 0.03 nm/μmol L^{-1} of nitrites presented with colorimetric readouts based on smartphone-MATLAB algorithm calibration.

Contact lenses for tear collection in wearable devices, an interesting form of noninvasive sensor for tear fluid measurement, have been developed. Wilson's group (57) designed the NovioSense glucose sensor for diabetes users to wear on the lower eyelid. The location of the device allows the wearable sensor to continuously measure the glucose level in the basal tear fluid. NovioSense consists of a three-electrode flexible coil with multiple wires wrapped in an amperometric cell. The outer surface of the device is coated with polysaccharide, reducing pain and irritating feelings for users. The sensor provides a stable glucose signal, and the results match the blood glucose level obtained from commercial blood measurements, where 92% of acquired data were in the A and B regions in the Clarke error grid analysis. However, the core design of the device is based on electrochemical response only. This device shows that the field of contact lenses as wearable microfluidic devices still lacks maturity and requires extensive improvements. In terms of sensitivity, biocompatibility, integration technology, product safety, and production cost, such platforms require further development to achieve practical applications.

2.4. Urine

Urine is not an emergent and typical sample for detection with wearable devices. There is some challenge in trying to monitor urine glucose levels. Zhang et al. (58) developed a flexible

self-powered sensing system integrated in a diaper for urine metabolite detection. The diaper system was powered by an enzymatic biofuel cell that utilized glucose composites in biofluid to convert the chemical energy of biofuel into electrical energy. The storage energy was used to drive a light-emitting diode (LED) flash that enabled the researchers to indicate the concentration of glucose in urine. The flashing frequency was proportional to the glucose concentration with an *R*-squared of 0.994 in the range of 1 to 5 mM. The self-powered wearable device could potentially be used in the control of urine glucose levels in diabetic patients with urinary incontinence.

2.5. Sweat

Sweat, secreted by eccrine or apocrine glands embedded in the human skin, contains various ionized particles and chemical biomarkers that are suitable for physiological condition analysis (59), such as electrolyte and alcohol levels (60). Sweat can also be used for clinical diagnosis, such as bone mineral loss (61), cystic fibrosis (62), and monitoring use of drugs such as cocaine (63). Compared to interstitial and blood detection by microneedle wearable devices, sweat analysis provides a noninvasive approach that is easier and safer for infants and elderly individuals.

The design of wearable microfluidic devices for sweat application can involve sweat harvesting, biomarker collection, and integration with further sensing techniques in one device. The common targets of sweat analysis include water (64), pH value (65–69), glucose (70–74), lactate (75, 76), Na^+ (77), K^+ (65), Cl^- (69), choline (74), hormone level (78, 79), levodopa (69), sweat secretion pressure (78, 80), and temperature (67) (**Figure 2**).

Nie et al. (68) fabricated a wearable integrated silicon sensor chip with a flexible laminated polyethylene terephthalate (PET) microfluidic device for sweat pH sensing. Cao et al. (70) demonstrated a three-dimensional, multilayer, paper-based microfluidic electrochemical integrated device (3D-PMED) for sweat glucose detection. The sweat sample was measured amperometrically in the range of 0 mM to 1.9 mM, with a sensitivity of 17.49 $\mu A/mM\ cm^2$. Yokus et al. (76) presented a wearable microfluidic patch that integrated hydrogel and filter paper for lactate detection. The patch detected the perspiration lactate level through electrochemical measurement, and the chronoamperometric measurement showed linear fitting in the range of 5 mM to 20 mM, with a sensitivity of 0.03 $\mu A/mM\ cm^2$. Martín et al. (71) presented a flexible microfluidic patch for rapid perspiration collection and lactate/glucose level detection. This flexible device can detect sweat lactate levels from 4 mM to 20 mM, with a relative standard deviation of 1.2% and a sensitivity of 29.6 $\mu M/\mu A$; it can also detect glucose levels from 2 mM to 10 mM with a relative standard deviation of 1.6%. Lin et al. (72) demonstrated thermoresponsive hydrogel valve–controlled wearable devices for programmable glucose and lactate sensing. The results showed a linear relationship between 50 μM and 400 μM glucose and 2 mM to 10 mM lactate. The authors fabricated a low-cost, 3D microfluidic structure with vertical interconnection for particle size selection and the detection of H_2O_2, glucose, and choline. A sandwich-like interface with simultaneous alternating current electrothermal (ACET) actuation was incorporated, and researchers noted a 47% enhancement of the H_2O_2 sensor current level, a 26% enhancement in sensitivity, and a 27% reduction of response time. With ACET, they revealed a 74% improvement of the glucose sensor current level, a 31% improvement in sensitivity, and a 33% reduction in response time. Similar trends were also found using the choline sensor (74).

Ma et al. (77) demonstrated a perspiration collecting and sensing wearable device composed of PET films and biocompatible threads. The perspiration was collected through capillary absorption by thread, and Na^+ was detected by embedded electrodes with a range of 10–160 mM. The Na^+ detection sensitivity was 59.8 mV in static mode and 56.7 mV in flow mode. The required time for thread-based microfluidic device fabrication is much less than that of polydimethylsiloxane (PDMS)-based devices (77). Zhang et al. (81) presented a smart battery-free wireless

K^+ ion detection wearable electrochemical sensing patch that collects sweat fluid for on-site monitoring. A hybridized multidimension network electrode with multiwalled carbon nanotubes and MXene was applied for superior electron transfer properties to achieve high-electroactivity performance. Microfluidic channel design led to a high-speed, smooth sweat flow at the inlet and outlet channels, facilitating an update of the detecting object but low flow speed at the electrochemical detection chamber for accurate analysis. The K^+ detection showed a high sensitivity of 63 mV/decade and amplified to 173 mV/decade with the integrated amplification system. Lee et al. (78) presented a stretchable, wearable, one-touch operation biosensor for perspiration cortisol level detection ranging from 1 pg/mL to 1 μg/mL. The average difference between the wearable biosensor and standard enzyme-linked immunosorbent assay results was 14.7%, and the sensitivity was 0.273 ohm mL/ng (78). Recently, Gao and colleagues (79) investigated a graphene-based stress-sensing platform for real-time hormone variation in sweat. Cortisol was detected through a competitive immunosensing reaction with horseradish peroxidase (HRP)-labeled cortisol at concentrations ranging from 0 to 10 ng/mL with up to 1 min of assay time. The trial results showed a strong correlation between serum cortisol levels and device detection in this study. Choi et al. designed a soft, skin-mounted patch for sweat secretory pressure measurement (82), sweat collection and storage (83), and further sweat rate and biochemical detection through colorimetric change (84).

Koh et al. (64) developed an integrated device containing four separate reservoirs and one serpentine microfluidic channel for isolated detection to prevent cross-contamination. A 5–10-μL sweat sample was needed for each reservoir, and the response time was less than 1 min for chloride, glucose, pH value, and lactate detection through colorimetric analysis. Vinoth et al. (65) developed a fully printed multifunctional wearable microfluidic chip to analyze electrolyte concentrations, including Na^+, K^+, lactate, and pH from collective sweat. The device specifically modified the initial layer with carboxylic acid–functionalized, single-walled carbon nanotubes (SWCNTs-COOH) and utilized Prussian blue nanoparticles to improve catalytic activity and sensing ability. The minimal sweat volume to fill the microfluidic chamber was 0.792 μL with a response time of 10 s for the electrolyte and 60 s for the lactate steady-state sensor response. Lactate with an LRR ranged from 1 to 25 mM. Xuan et al. (67) integrated the detection of pH value, lactate, and body temperature in one wearable device. The outer polymetric layers as diffusion-limiting layers modulated lactate flux and enabled an LRR from 1 to 50 mM with response times <5 s and less interference in pH value and temperature.

However, humans at rest may have a slow rate of sweat generation, which is not suitable for sweat collection and sensing. Most wearable microfluidic devices for sweat detection require subjects to perform continuous exercise for sweat collection (81, 85). Exercise such as cycling, stair climbing, treadmill running/walking, and swimming can increase sweat production. To perform collection and analyses of sweat from swimming, Reeder et al. (86) introduced a soft, skin-mounted, waterproof wearable patch that monitors hydration metrics in real time during aquatic sports. The wearable system combined with skin-compatible microfluidic networks measures the local sweat rate, sweat loss, and chloride concentration through colorimetric analysis. The adhesion of the wearable patch causes tight bonding to the skin for more than 2 h under intense underwater operation. The microfluidic system is also integrated with waterproof, flexible electronic devices, including a magnetic loop antenna, near-field communication component, and LED notification light to transmit digital identification codes for skin temperature to the smartphone system.

In addition to exercise, iontophoresis can be used to stimulate sweat production and has potential for general health care applications (67, 79). Saha et al. (75) developed a microfluidic device for long-duration sweat harvesting of approximately 12 h that is suitable for both resting

and active perspiration. Nyein et al. (69) developed a wearable device for resting sweat collection, sweat rate detection, and element sensing, including pH, chloride, and levodopa. The device contained a polyvinyl alcohol–coated patterned SU8 as a hydrophilic filler and agarose-glycerol film for rapid sweat absorption and transportation while maintaining its mechanical structure. The spiral channel facilitated sweat drawing and wheel-shaped electrode detection. The device could detect a flow rate as low as 2 nL/min.

3. FUNCTIONAL MICROFLUIDIC DESIGN

With the innovations in wearable sensing platforms of materials and designed manufacturing, the combination of fluid regulation and flexible electronics represents an advanced approach in personalized health care applications. Microfluidics realizes the general advantages in more function and design structures with proper biofluid collection, sample transfer, and detection performance.

3.1. Biofluid Collection and Storage

Traditional biofluid collection processes, such as blood drawing, collect biofluid through invasive procedures assisted by medical staffs at clinics. Biofluids that cannot be collected efficiently, such as perspiration, tears, and saliva, are not suitable for traditional biofluid examinations. In contrast, wearable microfluidic devices collect biofluid efficiently through direct contact with local biofluid secretion sites and enhance biofluid transportation through microfluidic channel structures (87). The effective sampling process and required microscale sample volume greatly reduce the inconvenience of conventional collection. The advantages of wearable microfluidic devices also lead to an increased variety of applicable biofluids. The microfluidic composition of sensor devices facilitates biofluid capture, storage, and processing (88, 89). Ex situ detection continuously quantifies biofluids at both the physical and chemical levels to evaluate physiological conditions. To continuously capture fluids using microfluidic devices, several strategies are applied to sample biofluids. However, the traditional method of fluid collection in microfluidic platforms often involves complex modules and auxiliary pumping systems that are not suitable for portable wearable devices. Therefore, passive driving forces would be an effective approach for biofluid sampling with microfluidic devices (90). Beyond the natural pumping force from the secretion gland, biofluid can be collected through capillary force, osmotic pressure, and evaporation driving force for wearable microfluidic design (64, 91, 92). **Figure 3** illustrates the driving force of microfluidic wearable devices.

3.1.1. Capillary force. For most wearable microfluidic devices, capillary force plays a fundamental role in fluid transportation and collection. With a fitted and soft flexible microfluidic skin patch, perspiration biofluid is collected by capillary absorption and harvesting in the hydrophilic channel. Microfluidic sensors utilize capillary force to deliver liquids in a preestablished manner by exploiting surface tension through geometry and interface chemistry.

An additional layer of hydration interface, usually hydrogel or filter paper, attached to the human skin surface and the microfluidic inlet would create a continuous flow that greatly increases the sampling efficiency and assists fluid to pass through the sharp edge smoothly (68). Koh et al. (64) coated a thin layer of cobalt(II) chloride containing a polyhydroxyethylmethacrylate (pHEMA) hydrogel in a microfluidic channel as a colorimetric indicator for perspiration flow. The pHEMA hydrogel also facilitates the continuous flow of perspiration and reduces the influence of momentary flow fluctuations (70). Paper-based microfluidic channels are also applied to wearable devices and facilitate fluid flow through capillary forces. The wax-patterned filter paper directly shapes the desired microfluidic channels. Cao et al. (70) utilized paper folding to form a

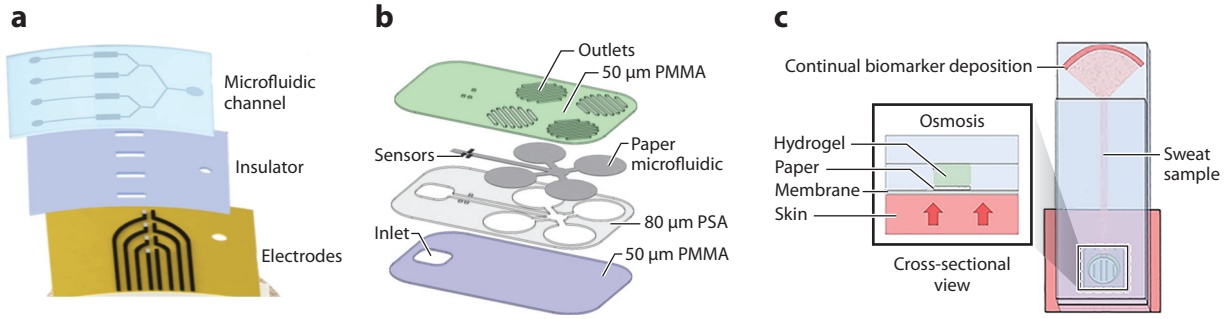

Figure 3

Wearable microfluidic devices to collect biofluid samples by applying different driving force. (*a*) A silicon rubber–based microfluidic channel assists the biofluid collection and drives biofluid flow by capillary force. Panel adapted with permission from Reference 65; copyright 2021 American Chemical Society. (*b*) A PMMA-based device assists biofluid collection and transports biofluid through capillary force provided by paper-based microfluidic channels. Panel adapted from Reference 85 (CC BY 4.0). (*c*) A microfluidic device collects and transports biofluid via a combination of capillary force, osmotic pressure, and evaporation. Biomarkers are deposited at the evaporated region for further analyses. Panel adapted with permission from Reference 75; copyright 2021 American Chemical Society. Abbreviations: PMMA, poly(methyl methacrylate); PSA, pressure sensitive adhesive.

3D microfluidic channel to direct perspiration flow and sensing in the vertical direction. Anastasova et al. (85) developed a hybrid microfluidic device incorporating a paper microfluidic channel to ensure absorption and sweat collection from skin. Integration of paper microfluidics with other microfluidic systems ensures continuous biofluid flow (75, 76). In addition to paper-based microfluidics, other materials, such as thread, can also be merged in the microfluidic sandwich system to collect biofluid through capillary force and deliver the biofluid to the sensing place (77). An absorbent fiber placed properly in the microfluidic channel can also provide a guide function to lead sweat into the sensing area (93).

3.1.2. Evaporation. Some studies utilize evaporation-driven forces for the power of continuously flowing pumping sources. Nie et al. (68) reported a continuous sweating device in which the sweat collector is made of three layers of PET. The fluidic inlet is integrated with a layer of filter that absorbs biofluid into the inlet. The capillary-driven biofluid fills the microchannel, passes through the sensing cavity, and reaches the porous outlet. Liquid evaporation through the pores generates continuous flow throughout the device without the involvement of an external pumping system. The 3D-PMED microfluidic channel presented by Cao et al. (70) was made of waxed cellulose paper with a stacked layer composed of a sweat collector, vertical channel, transverse channel, electrode layer, and sweat evaporator. The filter paper and hydrophobic waxed wall collected the sweat through capillary force, and the sweat flow was driven by sweat evaporation.

3.1.3. Osmotic pressure. The osmotic pressure between the hydration interface and biofluid extracts the fluid into the layer and pumps the fluid into the microfluidic channel. A specially designed high-concentration solute hydrogel can increase the osmotic pressure to facilitate biofluid flow through solute release. The osmolytes of hydrogels can be sodium chloride (73, 75), glucose (75, 76), and glycerol (73, 75), which should not interfere with the final biomarker detection depending on the sensing target. Acrylamide with a crosslinker such as *N*,*N*′-methylenebisacrylamide and a photoinitiator such as 2-hydroxy-4′-(2-hydroxyethoxy)-2-methylpropiophenone are widely used as a hydrogel in studies (73, 75, 76). Shay et al. (73) demonstrated a noninvasive collection and manipulation strategy for sweat sampling using a thin

layer of hydrogel patch with high solute immersion integrated into the microfluidic channel. The high ion level of the hydrogel drives the flow across the water-permeable membrane as simulated skin through osmotic pressure, creating a continuous fluid. This device can pump an accurate concentration of glucose solution through the membrane to the reservoir for further sensing.

3.1.4. Combined driving force. By combining osmotic pressure, capillary-driven forces, and evaporation-driven forces, the microfluidic biofluid collection device can passively generate continuous flow for a long time. Yokus et al. (76) presented a wearable sensing patch for sweat extraction and quantitative detection through capillarity, osmotic pressure, and evaporation forces. The hydrogel patch–contacted, paper-based microfluidic device was coupled in the system, resulting in the transportation of the biofluid. The screen-printed electrode was coupled to the microfluidic channel for the enzymatic electrochemical detection of lactate concentration. The evaporation region provided further drive power for continuous perspiration flow. Saha et al. (75) reported a sweat harvesting system for low-sweat-rate testing during natural human perspiration. The in vitro and in vivo sweat sampling processes involved capillarity, osmotic pressure, and evaporation. Sweat was first introduced to the microfluidic device through osmotic pressure via a hydrogel patch attached to the epidermal interface. Additionally, the interface of the hydrogel was in contact with the paper-based microfluidic channel, followed by the analysis zone and an evaporation pad. The fluid content was continuously transported from the analysis zone for 12 h, regulating the long-term extraction of sweat and metabolites.

3.2. Reservoirs, Valves, and Pumping

Multiple strategies can enhance biofluid collection and detection. To increase the compatibility of the contact surface, a flexible device is needed. By modifying the material component ratio, the microfluidic device can be flexible for better fitting but also has the potential for channel collapse. Micropillars within reservoirs (82, 83) and integrated separate stiffness layers can enhance the structural stability (71), whereas increasing the outlet number could effectively decrease the biofluid collection duration.

Most wearable microfluidic sensors are demonstrated through electrochemical or colorimetric sensing strategies for on-body physiological condition measurement. These wearable sensors usually rely on the passive collection of all kinds of biofluids. Valving the structure is fundamental to enhance the application flexibility and diversity of bioanalysis in wearable devices. An additional valve system controls the flow rate and direction, assisting analyte capture and readout. Choi et al. (82) fabricated a soft skin-mounted microfluidic patch with capillary bursting valves (CBVs) to measure sweat secretory pressure. The design included three poles in reservoirs for preventing collapse. One design included several separate microreservoirs with different individual microfluidic widths for sweat secretory pressure measurement. Another CBV design included sequential CBVs for sweat collection, storage, and further biomarker analysis (83). **Figure 4*b*** shows the collection of perspiration sequentially with controlled CBVs. When sweat first bursts through the CBV, it flows into microreservoir 1. After microreservoir 1 is filled, the sweat contained in the reservoir raises fluid pressure and subsequently flows through the CBV into microreservoir 2. By analogy, the sweat fills each CBV in order, flows through the long channel to each chamber, and presents the sweat pressure according to the filled chamber number. Three additional microfluidic channels that follow each CBV were designed for sweat collection and analyses after centrifugation. The same group reported soft, skin-interfaced multifunctional microfluidic platforms with optimized CBVs for stable glucose, pH, ion, and temperature level measurements in a broad range of ambient conditions (84). The CBV directed the sweat fluid to an individual colorimetric assay for separation chemical assessments, avoiding cross contamination.

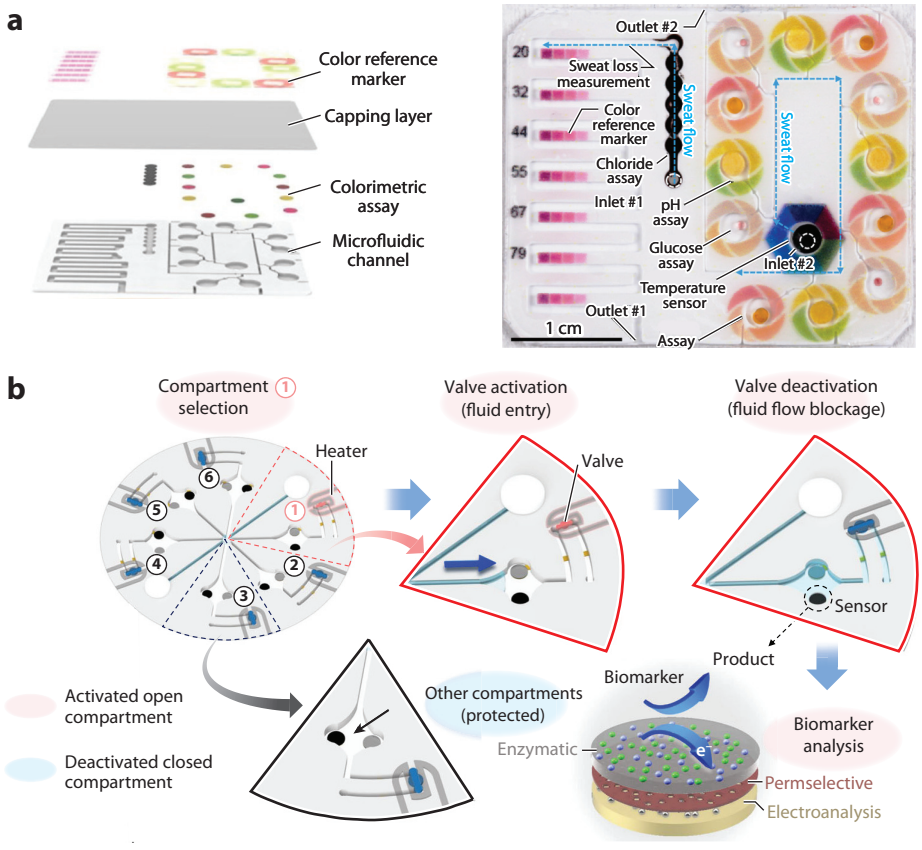

Figure 4

Valve-controlled design of microfluidic wearable devices. (*a*) CBV-controlled system for multiple biomarker sensing. The microfluidic valve system guides the sweat flow into detective wells with different colorimetric assays sequentially. The color reference markers near the detective wells assist the colorimetric result interpretation. Panel adapted with permission from Reference 84; copyright 2019 American Chemical Society. (*b*) Programmed biomarker sensing system controlled by thermoresponsive PNIPAM-based hydrogel valves. While the microheaters increase the temperature, the valves will shrink due to water released from the hydrogel and allow fluid entry. The circled numbers 1–6 represent each compartment with different biomarker sensors. Biomarkers in sweat can be detected by biomarker sensors in the channels, and the signal can be processed by the circuit board. When the microheaters selectively activate different compartment valves, the device can be programmed to sense specific sweat biomarkers accordingly. Panel adapted from Reference 72 (CC BY-NC 3.0). Abbreviations: CBV, capillary bursting valve; PNIPAM, poly(*N*-isopropylacrylamide).

Lee et al. (78) designed a passive microfluidic sample handling wearable patch sensor that integrated with a stretchable impedimetric sensing platform. The stretchable patch can precisely collect and transport sweat by one-touch operation reagent delivery to quantify cortisol. The microfluidic sensor comprises two layers of soft, stretchable PDMS. The sweat is passively absorbed into the inlet and incubated for 15 min in the sensing chamber. The preencapsulated reagent was burst into the sensing chamber through the CBV valve when the reagent chamber button was pressed for operation. The integrated wearable patch quantified sweat cortisol simultaneously with electrochemical signals during exercise.

Lin et al. (72) reported an active, programmable microfluidic valving system for biofluid collection for handling and compartmentalization in biomarker analysis. The wearable device contained six pressure-regulated compartment systems that were individually controlled by the thermoresponsive poly(*N*-isopropylacrylamide) (PNIPAM) hydrogel. The designed circuit-controlled micropatterned heater actuated the volumetric thermal response of the PNIPAM hydrogel and harvested biofluid sample compartmentalization at scheduled times and on demand. The membrane filter was integrated at the auxiliary microfluidic channel as a pressure regulation membrane to accommodate the pressure buildup while collecting sweat on the skin interface. The platform is capable of analyzing sweat-relevant biomarkers, such as glucose and lactate levels, based on on-body readouts. Multiple thin layers of microfluidic channels were assembled to provide vertical interconnection access for microfluidic flexible and complex extension (74). **Figure 4** shows the valve structures assisting flow control and analyte sensing.

3.3. Performing Detection

For conventional biomarker examinations, more than 5 mL of target biofluids are often required to perform the test. Hours to days are required to generate the formal reports. The wearable microfluidic devices integrate the biofluid collection and detection systems in one device to provide an immediate biomarker analysis. The detection systems utilize different types of sensors according to characteristics of the target objects. Both colorimetric sensors and electrochemical sensors are frequently applied for fast detection. The responding time, detection range, and strength of the result signal are the focus of wearable microfluidic sensor inventions.

3.3.1. Colorimetric sensing. Colorimetric sensing is one of the most widely used analytical technologies in biofluid metabolite detection. The colorimetric strategy relies on the analyte concentration and color intensities of the chemical element or chemical compound. Target analytes react with the sensing reagent, generating specific chemical reactions that change the color. To quantify the concentration of the target biomarker, the color change and intensity are detected using optical equipment. The cost of the colorimetric wearable device is relatively low, and most of the chip is disposable. However, the simplicity and intuitive measurement make colorimetric detection suitable for threshold warning indicators during daily life or in personal health care systems. The targets of colorimetric detection in wearable microfluidic devices include water (83), glucose (54, 84), lactate (64, 84), chloride (84, 86), pH value (28, 93), temperature (84, 86), protein (55), nitrite (55, 56), uric acid (56), and urea (54) in biofluid.

Colorimetric detection provides an intuitive, simple strategy for biofluid measurement. The presentation of the target analytes could even be obtained by naked-eye observation or digital image analysis software in smartphones. Such a convenient approach is widely used in athletic competition or fitness training. Koh et al. (64) demonstrated a soft wearable patch for sweat collection and storage for biochemical, electrolyte, and metabolite analysis through colorimetric detection. The wearable patch introduced sweat from skin and captured samples into microchannel networks connected to four circular chambers as biofluid reservoirs. Each reservoir contained a color response reagent that enabled the assessment of the pH value and selected metabolites, including glucose, lactate, and chloride ($CoCl_2$). Cobalt(II) and $CoCl_2$ contained in a coating of a pHEMA hydrogel matrix were patterned in microfluidic channels as a colorimetric indicator of water in sweat. The wearable patch is also integrated with near-field communication electronics that allow the wireless launch of image capture and digital analysis through a personal smartphone system. Hydrogels containing $CoCl_2$ are widely utilized for flow sensors (82, 83). In addition to $CoCl_2$, violet AmeriColor Soft Gel Paste (86) and dried food dye (71) were also

applied to water detection in wearable devices. Bromocresol purple, bromothymol blue, methyl red, and phenolphthalein are common reagents for pH value detection.

The biomarker level can also be detected through enzymatic reactions with cooperative cofactors and chromogenic reagents. For lactate detection, the interaction among lactate oxidase, nicotinamide adenine dinucleotide, and diaphorase leads to a color change in formazan. Glucose detection can be performed through prefixed glucose oxidase and iodide. The hydrogen peroxide (H_2O_2) produced by glucose oxidation induces iodide oxidation to iodine and changes the color from yellow to brown (64). Moreddu et al. (55), however, chose 3,3′,5,5′-tetramethylbenzidine to be oxidized with H_2O_2 and produced a color change from yellow to green for glucose level detection. The presented devices utilized 3′,3″,5′,5″-tetrachlorophenol-3,4,5,6-tetrabromosulfophthalein for protein detection and a mixture of 3-hydroxy-1,2,3,4-tetrahydro-7,8-benzoquinoline and sulfanilamide for nitrite detection.

The colorimetric method often has difficulty measuring biomarkers at low concentrations in sweat fluid. Most colorimetric wearable devices focus on chloride and lactate because of the high content in sweat fluid. The easiest way to test the readout result is by directly observing the color change with the naked eye. Images are captured through smartphones, and the RGB level of color presentation is analyzed through software to assist in target concentration recognition. Other optical sensing technologies, such as fluorescence sensing probes, could enhance the sensitivity and selectivity targeting low levels of biomarkers. Benito-Lopez et al. (93) chose bromocresol purple as a pH-sensitive dye and detected the color through a pair of μ-LEDs. Black masking tape was required in the device to mask ambient light to enable enhanced precise color detection.

3.3.2. Electrochemical sensing. Integrating electrochemical sensors with microfluidics in wearable sensors is an attractive approach in biofluid sampling, biomarker analysis, and noise minimization. The electrode is a fixed biosensitive material including antibody, enzyme, peptide, or mediator to react with the target molecules, generating electrical signals for the target quantification analysis. Biochemical data are captured and transmitted into digital forms and can be recorded and analyzed through wireless transmittance for further biomarker monitoring. The targets of electrochemical detection in wearable microfluidic devices include glucose (72, 74), lactate (76, 85), choline (74), Na^+ (85), K^+ (81), Cl^- (69), pH (85), levodopa (69), and cortisol levels (78) in biofluid.

Potentiometric electrodes featuring ion-selective membranes are suitable for electrolyte detection, such as Na^+, K^+, Cl^-, and pH values. Enzymatic oxidation with an efficient redox mediator–coated electrode with amperometric detection is suitable for lactate and glucose detection. Prussian blue (PB) can selectively recognize H_2O_2 and is widely applied to various oxidase enzyme–based analyses. A nonparticle form of PB enhances the catalytic and sensing ability (65). PB combined with lactate oxidase provides a convenient tool for lactate detection (65, 67, 70). Glucose levels can be measured through glucose oxidase in cooperation with PB (70, 71). However, Lin et al. (72) utilized lactate oxidase coated on a poly(*m*-phenylenediamine) (PPD)/platinum nanoparticle (PtNP)/Au electrode as a lactate sensor and glucose oxidase coated on a PPD/PtNP/Au electrode as a glucose sensor. Kim et al. (53) reported soft, multifunctional contact lenses for the electrochemical detection of glucose and IOP in tears. The glucose sensor is based on a field-effect transistor that consists of a graphene channel hybrid with Ag nanowires. Glucose oxidase was immobilized on the electrode through a pyrene linker and catalyzed the oxidation of glucose, generating H_2O_2 so that the current change could be detected. Simultaneous ACET by Lin et al. (74) enhanced H_2O_2 sensing, including the current level and sensitivity, and reduced the response time. Because H_2O_2 plays an important role in general enzymatic sensing, simultaneous ACET revealed similar effects on glucose and choline detection through glucose oxidase and choline oxidase.

To extend the LRR in lactate detection, Xuan et al. (67) incorporated diffusion-limiting membranes at the outer layer of the PB-Lox electrode. Different polyvinyl chloride (PVC) membranes were compared, and the PVC/DOS/ETH500 membrane with a 3 wt% content of ETH500 was chosen for a wider LRR and reproducible response. The diffusion-limiting layers modulated lactate flux and enabled an increase in LRR from 1 to 50 mM with response times <5 s and less pH value and temperature interference.

For hormone level measurement, anticortisol antibody is utilized for sweat cortisol level measurement. Lee et al. (78) developed a four-chamber microfluidic system with bursting valve control to detect cortisol levels in sweat with a cortisol antibody. The device measured cortisol concentration through electrochemical impedimetric spectroscopy and utilized 3D nanostructured Au to increase sensitivity with a measurement range of 1 pg/mL to 10 ng/mL. In research by Gao et al. (94), graphene-based electrodes were utilized for superior electrochemical sensing. The key stress hormone cortisol is recognized by the anticortisol antibody that is immobilized on the graphene-based electrode, competing with the HRP-labeled cortisol. Reduction of the H_2O_2 that is generated by the HRP creates the cathodic current measured by the amperometric response, which is proportional to the concentration of cortisol in sweat. To enhance the sensitivity of electrochemical sensing, Lee et al. (78) fabricated a working electrode with 3D nanostructured Au to increase the reaction surface area and maximize the reaction signal. To record the current and resistance change from the electrochemical response and proceed with further data analysis, data transmission with/without wire is required for the devices.

3.4. Mechanical Sensing

Both biophysical and biochemical integrated sensors are important to obtain a whole picture of an individual's dynamic health condition. Most microfluidic wearable devices target biochemical signals, including metabolites, antibodies, and enzymes, but biophysical signals are also important for assessing physiological conditions. Mechanical-based wearable sensors are different aspects that transfer physiological, physical, or chemical information into mechanical signals, linking the gap between biomarkers and mechanical signals to the real-time microscale of induced bioreactions. Mechanical-based wearable devices generally focus on the microfluidic pressure, strain, deformation, and swelling effect.

The biofluid-based microfluidic sensor offers a suitable approach for detecting tissue pressure that is correlated to human physiological activity. Conventional liquid-based microfluidic sensors collect working fluid in the microfluidic channel. Lin et al. (80) presented a noninvasive headband that continuously measures secretion sweat pressure during exercise. Secretion pressure is detected by a one-inlet pneumatic microfluidic chip in which the applied fluid enters the inlet and is forced to cease in a certain position of the microchannel depending on the compression of the sealed air volume. Sweat pressure is detected by the change in resistance from the pair of electrode patterns, and the signal is transported to a personal smartphone for real-time display. In the human trial, the wearable device showed a range of 1.3 to 2.5 kPa in different exercise activities. Another example of sensing sweat pressure through a microfluidic structure was demonstrated by Rogers and colleagues (82). They presented a soft, skin-mounted patch that contains 12 pressure-sensing chambers. Each chamber was controlled by the CBV with different bursting pressures. While the applied sweat pressure exceeded the bursting pressure, sweat flowed into the chamber, changing the indicator from blue to pink. The colorimetric changes showed the maximum sweating pressure during the entire exercise process. The average range of healthy adults is 2.4 to 2.9 kPa in human exercise demonstrations. **Figure 5** shows microfluidic wearable devices for pressure measurement.

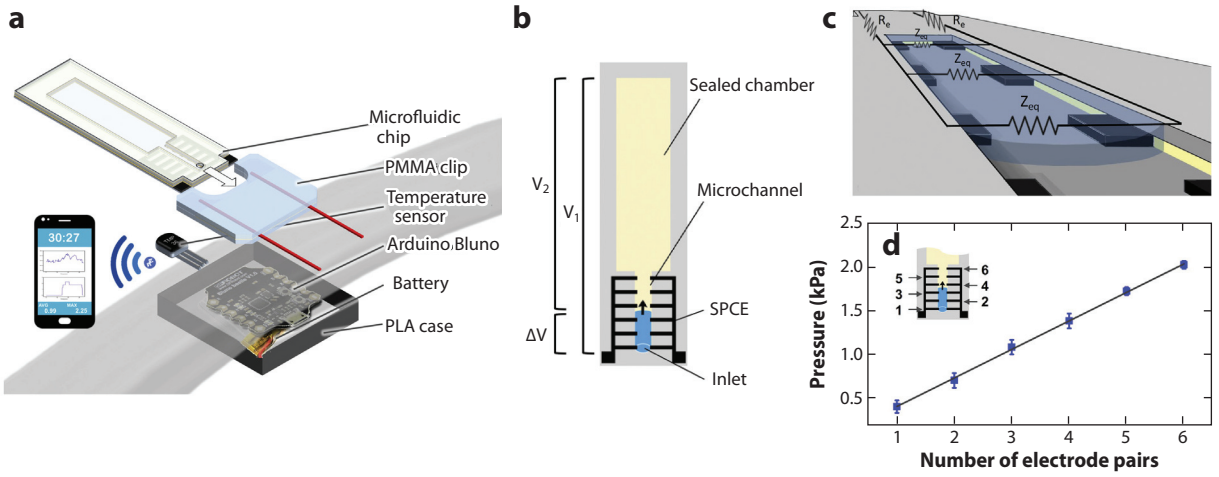

Figure 5

Wearable microfluidic devices for pressure measurement. A headband microfluidic device with six paired SPCEs measures perspiration pressure through detecting the resistance variance signals. (*a*) The microfluidic chip embedded in the headband device measures the perspiration pressure and transmits the signal to a smartphone via Bluetooth. (*b*) Sensing chip design. The sealed pneumatic microchannel chamber contains the original volume of air (V_1). While perspiration flowed into the chamber, perspiration pressure is balanced with the compressed air pressure in the sealed chamber with compressed volume (V_2). The perspiration pressure can be deduced based on the ideal gas law with variance of the trapped air volume, temperature, and atmospheric pressure. (*c*) The entry perspiration wets the parallel electrode pairs and the liquid–electrode interface forms interface resistance. The Z_{eq} can be detected and used for volume determination and pressure calculation. (*d*) Graph shows the corresponding pressure value to the liquid–electrode interface location. Panel adapted with permission from Reference 80; copyright 2020 Cell Press. Abbreviations: PLA, polylactic acid; PMMA, poly(methyl methacrylate); R_e, impedance of electrodes; SPCE, screen-printed carbon electrode; Z_{eq}, equilibrium solution impedance.

Mechanical sensing is also applied to IOP detection. Corneal curvature change caused by IOP change leads to mechanical strain of the microfluidic devices. The mechanical strain of contact lens-based microfluidic devices resulted in volume expansion and compression of the indicator liquid in a closed microfluidic channel. Through different microfluidic channel designs, the IOP can be measured via a clock-like indicator (50) and loop indicators (52). Kim et al. (53) also detected IOP through contact lens–based wearable microfluidic devices. They placed a layer of silicone elastomer between two spiral electrodes fabricated by graphene-Ag nanowires. The applied IOP increased the corneal radius curvature. The curvature change caused lateral expansion of the spiral coil and thinning of the dielectric. The change leads to an increase in the capacitance and inductance and results in the shifting of the spiral antenna to a lower frequency. **Figure 6** shows contact lens–based microfluidic devices for IOP measurement.

In addition to measuring sweat pressure, the wearable microfluidic device also measures intraabdominal pressure. Jiang et al. (95) reported an implantable microfluidic-based pressure wearable device for the sensing of intraabdominal pressure. The microfluidic device contains a pressure-sensitive membrane that covers the microfluidic chamber filled with water. When abdominal pressure is applied, the membrane deflects and pushes the water into the sensing channel, where the water position indicates the internal pressure. The water location is quantitively measured by the 40-MHz ultrasound imaging system. The sensing pressure could range from 0 to 12.6 kPa, showing a linear response of 42 kPa/mm and remaining functional after more than 600 cycles of pressure sensing for two days.

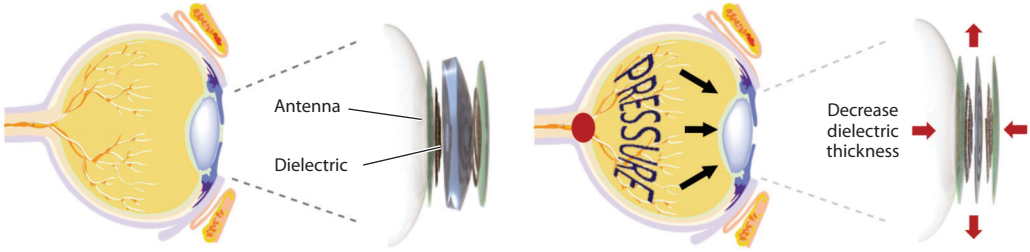

Figure 6

Microfluidic devices for intraocular pressure measurement. Increased intraocular pressure causes expansion of corneal surface curvature, which leads to frequency change induced by antenna shifting. The red arrows demonstrate the decreased dielectric thickness and biaxial lateral expansion of the spiral coils. Figure adapted from Reference 53 (CC BY 4.0).

With a simple design, a colorimetric microfluidic channel can be used to record sweat loss and sweat rate through sweat-filled microfluidic channel volume and time interval calculations (84). Nyein et al. (69) demonstrated a wearable device for sweat rate measurement under a low flow rate. The device features a spiral microfluidic channel and wheel-shaped electrodes. While sweat flows along with the spiral microfluidic channel, the impedance decreases with each fluid contact. The sweat rate can be calculated by counting the number of impedances, decreasing pulse, and the correlated time interval (**Figure 7**).

However, Reeder et al. (86) measured the collected sweat volume by counting filled serpentine microfluidic channels. Sweat loss and sweat rate were calculated by measuring the weight change of the absorbent foam pad near the microfluidic device and comparing it to the body weight loss percentage. With the use of filter paper in microfluidic channels, microfluidic devices can be utilized for particle selection (74).

4. PERSPECTIVES AND CONCLUSIONS

The integration of microfluidics and wearable devices is an excellent development in health care applications owing to several inherent advantages. First, microfluidic channels can gather on-chip a certain amount of liquid for high-accuracy measurement. Effective low-volume collection is particularly beneficial for sampling biofluid, which is often secreted in limited amounts. The low-volume features not only reduce the burden on individuals but also increase the range of application of wearable devices. Second, microfluidics shows great versatility when integrated with different detection systems, as it is easily combined with different detection methods with multiple targets. Even different electronic modules can be realized in multifunctional wearable sensing arrays. Third, the microfluidics channel exhibits good mechanical and adhesive properties. The design materials typically include polymer, silicon elastomer, and fabric, and the interface matches human skin well. These materials have an inherently low modulus that slightly deforms under small pressure application without detachment or breakdown. Because of their good compatibility with human skin, these materials act well as conduits for electronic modules in electrical connection approaches for further data acquisition. Fourth, cost of the microfluidic system is relatively low, and the system is easy to manufacture, leading to more convenience and feasibility for all users in the health care market.

The integration of microfluidic channels increases the application potential of wearable devices. Through delicate design, microfluidic channels and connected reservoirs act as a flow guide for biofluid collection and analyte sensing with multiple techniques on one device and

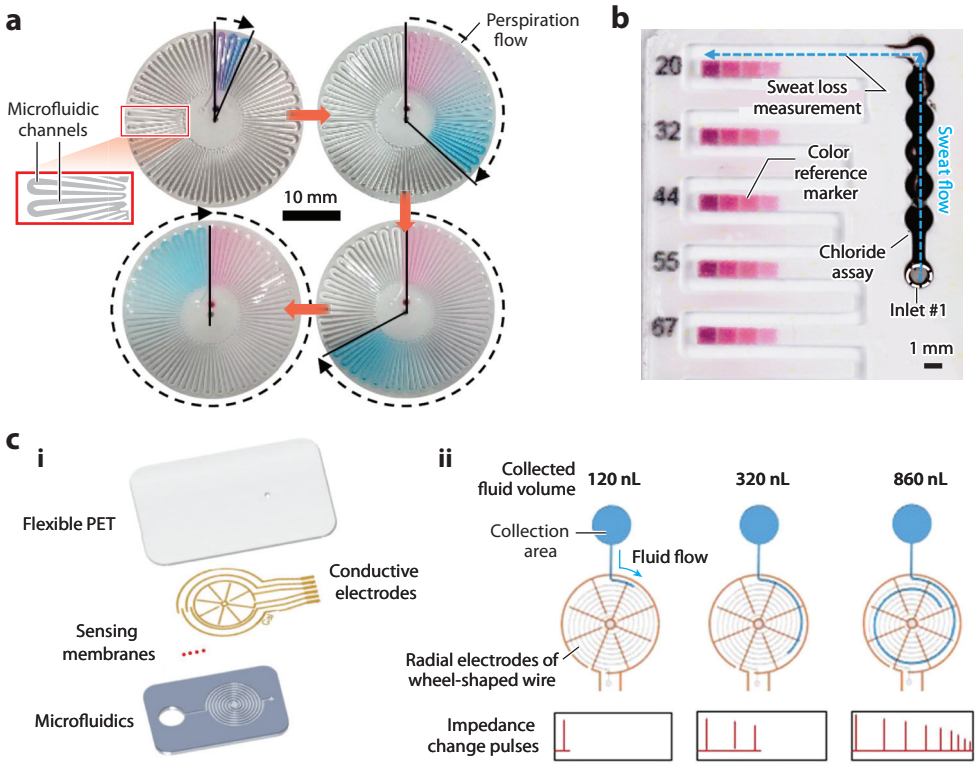

Figure 7

Microfluidic wearable devices for biofluid volume sensor and flow rate calculations. (*a*) Different rate water-soluble dyes in microfluidic channels (*pink* and *blue*) assist serpentine microfluidic channel number counting for perspiration volume prediction and flow rate calculation. Panel adapted from Reference 86 (CC BY-NC 3.0). (*b*) Color reference for perspiration volume loss measurement. Panel adapted from Reference 84 (CC BY 4.0). (*c*, *i*) The wearable patch is composed of a flexible polyethylene terephthalate (PET) layer, spiral microfluidic channels, and incorporated conductive electrode sensors. (*c*, *ii*) The microfluidic channel collects perspiration and transports it into spiral microfluidic channels. As the perspiration is transported forward, the fluid will contact the radial electrodes of wheel-shaped wire. Each electrode contacted by fluid causes impedance change (*top*). The more the perspiration is collected in the spiral channel, the more impedance change pulses can be detected (*red bars*) and used for flow volume estimation. The flow rate can be calculated by counting the impedance pulse number and time interval (*bottom*). Panel adapted from Reference 69 (CC BY 4.0).

without the concern of contamination. Microfluidic channels can be constructed in complex 3D structures for complicated biofluidic flow and sensing in both the horizontal and vertical directions, which facilitates volume reduction of the sensing device. With the integration of various materials in microfluidic channels, biofluid transportation can be enhanced by increasing the capillary force, hydrophilicity, and evaporated driving force. Microfluidic channels can be directly utilized for pressure sensors through architecture strain and flow rate calculations through cooperation with designed electrodes. The special valve design of the microfluidic channel allows pressure-controlled sequential flow and testing of biofluids in multiple applications. Compared to general wearable devices, microfluidic wearable devices are suitable for dexterous, complex, multifunctional sensor development.

DISCLOSURE STATEMENT

The authors are not aware of any affiliations, memberships, funding, or financial holdings that might be perceived as affecting the objectivity of this review.

ACKNOWLEDGMENTS

B.-R.L. acknowledges the support of Ministry of Science and Technology, Taiwan (grant no. NSTC 111-2221-E-A49-026) and the Center for Emergent Functional Matter Science of National Yang Ming Chiao Tung University from The Featured Areas Research Center Program within the framework of the Higher Education Sprout Project by the Ministry of Education in Taiwan.

LITERATURE CITED

1. Haghi M, Thurow K, Stoll R. 2017. Wearable devices in medical internet of things: scientific research and commercially available devices. *Healthc. Inform. Res.* 23:4–15
2. Takei K, Honda W, Harada S, Arie T, Akita S. 2015. Toward flexible and wearable human-interactive health-monitoring devices. *Adv. Healthc. Mater.* 4:487–500
3. Wu M, Luo J. 2019. Wearable technology applications in healthcare: a literature review. *Online J. Nurs. Inform.* 23. **https://www.himss.org/resources/wearable-technology-applications-healthcare-literature-review**
4. Iqbal S, Mahgoub I, Du E, Leavitt MA, Asghar W. 2021. Advances in healthcare wearable devices. *NPJ Flex. Electron.* 5:9
5. Erdem Ö, Derin E, Shirejini SZ, Sagdic K, Yilmaz EG, et al. 2022. Carbon-based nanomaterials and sensing tools for wearable health monitoring devices. *Adv. Mater. Technol.* 7:2100572
6. Godfrey A, Hetherington V, Shum H, Bonato P, Lovell N, Stuart S. 2018. From A to Z: wearable technology explained. *Maturitas* 113:40–47
7. Kireev D, Sel K, Ibrahim B, Kumar N, Akbari A, et al. 2022. Continuous cuffless monitoring of arterial blood pressure via graphene bioimpedance tattoos. *Nat. Nanotechnol.* 17:864–70
8. Sujith A, Sajja GS, Mahalakshmi V, Nuhmani S, Prasanalakshmi B. 2022. Systematic review of smart health monitoring using deep learning and artificial intelligence. *Neurosci. Inform.* 2:100028
9. Promphet N, Ummartyotin S, Ngeontae W, Puthongkham P, Rodthongkum N. 2021. Non-invasive wearable chemical sensors in real-life applications. *Anal. Chim. Acta* 1179:338643
10. Abdolmaleki H, Kidmose P, Agarwala S. 2021. Droplet-based techniques for printing of functional inks for flexible physical sensors. *Adv. Mater.* 33:2006792
11. Tzianni EI, Hrbac J, Christodoulou DK, Prodromidis MI. 2020. A portable medical diagnostic device utilizing free-standing responsive polymer film-based biosensors and low-cost transducer for point-of-care applications. *Sens. Actuators B* 304:127356
12. Shafiee A, Ghadiri E, Kassis J, Williams D, Atala A. 2020. Energy band gap investigation of biomaterials: a comprehensive material approach for biocompatibility of medical electronic devices. *Micromachines* 11:105
13. Nag A, Mukhopadhyay SC, Kosel J. 2017. Wearable flexible sensors: a review. *IEEE Sens. J.* 17:3949–60
14. Pavlov VA, Chavan SS, Tracey KJ. 2020. Bioelectronic medicine: from preclinical studies on the inflammatory reflex to new approaches in disease diagnosis and treatment. *Cold Spring Harbor. Perspect. Med.* 10:a034140
15. McGarraugh G, Bergenstal R. 2009. Detection of hypoglycemia with continuous interstitial and traditional blood glucose monitoring using the FreeStyle Navigator Continuous Glucose Monitoring System. *Diabetes Technol. Ther.* 11:145–50
16. Zhao M, Leung PS. 2020. Revisiting the use of biological fluids for noninvasive glucose detection. *Future Med. Chem.* 12:645–47
17. Lee I, Probst D, Klonoff D, Sode K. 2021. Continuous glucose monitoring systems—current status and future perspectives of the flagship technologies in biosensor research. *Biosens. Bioelectron.* 181:113054

18. Martens T, Beck RW, Bailey R, Ruedy KJ, Calhoun P, et al. 2021. Effect of continuous glucose monitoring on glycemic control in patients with type 2 diabetes treated with basal insulin: a randomized clinical trial. *JAMA* 325:2262–72
19. Bandari N, Dargahi J, Packirisamy M. 2019. Tactile sensors for minimally invasive surgery: a review of the state-of-the-art, applications, and perspectives. *IEEE Access* 8:7682–708
20. Lv C, Wang S, Shi C. 2020. A high-precision and miniature fiber Bragg grating-based force sensor for tissue palpation during minimally invasive surgery. *Ann. Biomed. Eng.* 48:669–81
21. Chen G, Zheng J, Liu L, Xu L. 2019. Application of microfluidics in wearable devices. *Small Methods* 3:1900688
22. Yang Y, Chen Y, Tang H, Zong N, Jiang X. 2020. Microfluidics for biomedical analysis. *Small Methods* 4:1900451
23. Lin P-H, Li B-R. 2021. Passively driven microfluidic device with simple operation in the development of nanolitre droplet assay in nucleic acid detection. *Sci. Rep.* 11:21019
24. Kilic T, Navaee F, Stradolini F, Renaud P, Carrara S. 2018. Organs-on-chip monitoring: sensors and other strategies. *Microphysiol. Syst.* 2:1–32
25. Sosa-Hernández JE, Villalba-Rodríguez AM, Romero-Castillo KD, Aguilar-Aguila-Isaías MA, García-Reyes IE, et al. 2018. Organs-on-a-chip module: a review from the development and applications perspective. *Micromachines* 9:536
26. Kumar A, Parihar A, Panda U, Parihar DS. 2022. Microfluidics-based point-of-care testing (POCT) devices in dealing with waves of COVID-19 pandemic: the emerging solution. *ACS Appl. Bio Mater.* 5:2046–68
27. Lee H, Hong YJ, Baik S, Hyeon T, Kim D-H. 2018. Enzyme-based glucose sensor: from invasive to wearable device. *Adv. Healthc. Mater.* 7:1701150
28. Madden J, O'Mahony C, Thompson M, O'Riordan A, Galvin P. 2020. Biosensing in dermal interstitial fluid using microneedle based electrochemical devices. *Sens. Bio-Sens. Res.* 29:100348
29. Samant PP, Prausnitz MR. 2018. Mechanisms of sampling interstitial fluid from skin using a microneedle patch. *PNAS* 115:4583–88
30. Tran BQ, Miller PR, Taylor RM, Boyd G, Mach PM, et al. 2018. Proteomic characterization of dermal interstitial fluid extracted using a novel microneedle-assisted technique. *J. Proteome Res.* 17:479–85
31. Zhang J, Bhattacharyya S, Hickner RC, Light AR, Lambert CJ, et al. 2019. Skeletal muscle interstitial fluid metabolomics at rest and associated with an exercise bout: application in rats and humans. *Am. J. Physiol. Endocrinol. Metab.* 316:E43–53
32. Thennadil SN, Rennert JL, Wenzel BJ, Hazen KH, Ruchti TL, Block MB. 2001. Comparison of glucose concentration in interstitial fluid, and capillary and venous blood during rapid changes in blood glucose levels. *Diabetes Technol. Ther.* 3:357–65
33. Kim J, Sempionatto JR, Imani S, Hartel MC, Barfidokht A, et al. 2018. Simultaneous monitoring of sweat and interstitial fluid using a single wearable biosensor platform. *Adv. Sci.* 5:1800880
34. Isensee K, Müller N, Pucci A, Petrich W. 2018. Towards a quantum cascade laser-based implant for the continuous monitoring of glucose. *Analyst* 143:6025–36
35. Ranamukhaarachchi SA, Padeste C, Dübner M, Häfeli UO, Stoeber B, Cadarso VJ. 2016. Integrated hollow microneedle-optofluidic biosensor for therapeutic drug monitoring in sub-nanoliter volumes. *Sci. Rep.* 6:29075
36. Jina A, Tierney MJ, Tamada JA, McGill S, Desai S, et al. 2014. Design, development, and evaluation of a novel microneedle array-based continuous glucose monitor. *J. Diabetes Sci. Technol.* 8:483–87
37. Chang P-H, Weng C-C, Li B-R, Li Y-K. 2020. An antifouling peptide-based biosensor for determination of *Streptococcus pneumonia* markers in human serum. *Biosens. Bioelectron.* 151:111969
38. Lin T-Y, Li B-R, Tsai S-T, Chen C-W, Chen C-H, et al. 2013. Improved silicon nanowire field-effect transistors for fast protein–protein interaction screening. *Lab Chip* 13:676–84
39. Li B-R, Hsieh Y-J, Chen Y-X, Chung Y-T, Pan C-Y, Chen Y-T. 2013. An ultrasensitive nanowire-transistor biosensor for detecting dopamine release from living PC12 cells under hypoxic stimulation. *J. Am. Chem. Soc.* 135:16034–37
40. Chen Y, Lu S, Zhang S, Li Y, Qu Z, et al. 2017. Skin-like biosensor system via electrochemical channels for noninvasive blood glucose monitoring. *Sci. Adv.* 3:e1701629

41. Bosch JA. 2014. The use of saliva markers in psychobiology: mechanisms and methods. *Saliva Secret. Funct.* 24:99–108
42. Lee Y-H, Wong DT. 2009. Saliva: an emerging biofluid for early detection of diseases. *Am. J. Dent.* 22:241–48
43. Kaufman E, Lamster IB. 2002. The diagnostic applications of saliva—a review. *Crit. Rev. Oral. Biol. Med.* 13:197–212
44. Wang A, Wang CP, Tu M, Wong DTW. 2016. Oral biofluid biomarker research: current status and emerging frontiers. *Diagnostics* 6:45
45. Zhang C-Z, Cheng X-Q, Li J-Y, Zhang P, Yi P, et al. 2016. Saliva in the diagnosis of diseases. *Int. J. Oral Sci.* 8:133–37
46. Arakawa T, Tomoto K, Nitta H, Toma K, Takeuchi S, et al. 2020. A wearable cellulose acetate-coated mouthguard biosensor for in vivo salivary glucose measurement. *Anal. Chem.* 92:12201–7
47. Lee Y, Howe C, Mishra S, Lee DS, Mahmood M, et al. 2018. Wireless, intraoral hybrid electronics for real-time quantification of sodium intake toward hypertension management. *PNAS* 115:5377–82
48. García-Carmona L, Martín A, Sempionatto JR, Moreto JR, González MC, et al. 2019. Pacifier biosensor: toward noninvasive saliva biomarker monitoring. *Anal. Chem.* 91:13883–91
49. Pankratov D, González-Arribas E, Blum Z, Shleev S. 2016. Tear based bioelectronics. *Electroanalysis* 28:1250–66
50. Agaoglu S, Diep P, Martini M, Samudhyatha KT, Baday M, Araci IE. 2018. Ultra-sensitive microfluidic wearable strain sensor for intraocular pressure monitoring. *Lab Chip* 18:3471–83
51. An H, Chen L, Liu X, Zhao B, Ma D, Wu Z. 2018. A method of manufacturing microfluidic contact lenses by using irreversible bonding and thermoforming. *J. Micromech. Microeng.* 28:105008
52. An H, Chen L, Liu X, Zhao B, Zhang H, Wu Z. 2019. Microfluidic contact lenses for unpowered, continuous and non-invasive intraocular pressure monitoring. *Sens. Actuators A* 295:177–87
53. Kim J, Kim M, Lee M-S, Kim K, Ji S, et al. 2017. Wearable smart sensor systems integrated on soft contact lenses for wireless ocular diagnostics. *Nat. Commun.* 8:14997
54. Yang X, Yao H, Zhao G, Ameer GA, Sun W, et al. 2020. Flexible, wearable microfluidic contact lens with capillary networks for tear diagnostics. *J. Mater. Sci.* 55:9551–61
55. Moreddu R, Wolffsohn JS, Vigolo D, Yetisen AK. 2020. Laser-inscribed contact lens sensors for the detection of analytes in the tear fluid. *Sens. Actuators B* 317:128183
56. Moreddu R, Nasrollahi V, Kassanos P, Dimov S, Vigolo D, Yetisen AK. 2021. Lab-on-a-contact lens platforms fabricated by multi-axis femtosecond laser ablation. *Small* 17:2102008
57. Kownacka AE, Vegelyte D, Joosse M, Anton N, Toebes BJ, Lauko J, et al. 2018. Clinical evidence for use of a noninvasive biosensor for tear glucose as an alternative to painful finger-prick for diabetes management utilizing a biopolymer coating. *Biomacromolecules* 19:4504–11
58. Zhang J, Liu J, Su H, Sun F, Lu Z, Su A. 2021. A wearable self-powered biosensor system integrated with diaper for detecting the urine glucose of diabetic patients. *Sens. Actuators B* 341:130046
59. Pilardeau P, Vaysse J, Garnier M, Joublin M, Valeri L. 1979. Secretion of eccrine sweat glands during exercise. *Br. J. Sports Med.* 13:118–21
60. Gamella M, Campuzano S, Manso J, Gonzalez de Rivera G, López-Colino F, et al. 2014. A novel non-invasive electrochemical biosensing device for in situ determination of the alcohol content in blood by monitoring ethanol in sweat. *Anal. Chim. Acta* 806:1–7
61. Klesges RC, Ward KD, Shelton ML, Applegate WB, Cantler ED, et al. 1996. Changes in bone mineral content in male athletes: mechanisms of action and intervention effects. *JAMA* 276:226–30
62. Ray TR, Ivanovic M, Curtis PM, Franklin D, Guventurk K, et al. 2021. Soft, skin-interfaced sweat stickers for cystic fibrosis diagnosis and management. *Sci. Transl. Med.* 13:eabd8109
63. Burns M, Baselt RC. 1995. Monitoring drug use with a sweat patch: an experiment with cocaine. *J. Anal. Toxicol.* 19:41–48
64. Koh A, Kang D, Xue Y, Lee S, Pielak RM, et al. 2016. A soft, wearable microfluidic device for the capture, storage, and colorimetric sensing of sweat. *Sci. Transl. Med.* 8:366ra165
65. Vinoth R, Nakagawa T, Mathiyarasu J, Mohan AMV. 2021. Fully printed wearable microfluidic devices for high-throughput sweat sampling and multiplexed electrochemical analysis. *ACS Sens.* 6:1174–86

66. Boria RA, Olson LE, Goodman SM, Anderson RP. 2014. Spatial filtering to reduce sampling bias can improve the performance of ecological niche models. *Ecol. Model.* 275:73–77
67. Xuan X, Pérez-Ràfols C, Chen C, Cuartero M, Crespo GA. 2021. Lactate biosensing for reliable on-body sweat analysis. *ACS Sens.* 6:2763–71
68. Nie C, Frijns A, Zevenbergen M, den Toonder J. 2016. An integrated flex-microfluidic-Si chip device towards sweat sensing applications. *Sens. Actuators B* 227:427–37
69. Nyein HYY, Bariya M, Tran B, Ahn CH, Brown BJ, et al. 2021. A wearable patch for continuous analysis of thermoregulatory sweat at rest. *Nat. Commun.* 12:1823
70. Cao Q, Liang B, Tu T, Wei J, Fang L, Ye X. 2019. Three-dimensional paper-based microfluidic electrochemical integrated devices (3D-PMED) for wearable electrochemical glucose detection. *RSC Adv.* 9:5674–81
71. Martín A, Kim J, Kurniawan JF, Sempionatto JR, Moreto JR, et al. 2017. Epidermal microfluidic electrochemical detection system: enhanced sweat sampling and metabolite detection. *ACS Sens.* 2:1860–68
72. Lin H, Tan J, Zhu J, Lin S, Zhao Y, et al. 2020. A programmable epidermal microfluidic valving system for wearable biofluid management and contextual biomarker analysis. *Nat. Commun.* 11:4405
73. Shay T, Dickey MD, Velev OD. 2017. Hydrogel-enabled osmotic pumping for microfluidics: towards wearable human-device interfaces. *Lab Chip* 17:710–16
74. Lin H, Zhao Y, Lin S, Wang B, Yeung C, et al. 2019. A rapid and low-cost fabrication and integration scheme to render 3D microfluidic architectures for wearable biofluid sampling, manipulation, and sensing. *Lab Chip* 19:2844–53
75. Saha T, Fang J, Mukherjee S, Dickey MD, Velev OD. 2021. Wearable osmotic-capillary patch for prolonged sweat harvesting and sensing. *ACS Appl. Mater. Interfaces* 13:8071–81
76. Yokus MA, Saha T, Fang J, Dickey MD, Velev OD, Daniele MA. 2019. *Towards wearable electrochemical lactate sensing using osmotic-capillary microfluidic pumping*. Presented at 2019 IEEE SENSORS, Montreal, Can., Oct. 27–30
77. Ma B, Chi J, Xu C, Ni Y, Zhao C, Liu H. 2020. Wearable capillary microfluidics for continuous perspiration sensing. *Talanta* 212:120786
78. Lee H-B, Meeseepong M, Trung TQ, Kim B-Y, Lee N-E. 2020. A wearable lab-on-a-patch platform with stretchable nanostructured biosensor for non-invasive immunodetection of biomarker in sweat. *Biosens. Bioelectron.* 156:112133
79. Torrente-Rodríguez RM, Tu J, Yang Y, Min J, Wang M, et al. 2020. Investigation of cortisol dynamics in human sweat using a graphene-based wireless mHealth system. *Matter* 2:921–37
80. Lin P-H, Chang W-L, Sheu S-C, Li B-R. 2020. A noninvasive wearable device for real-time monitoring of secretion sweat pressure by digital display. *iScience* 23:101658
81. Zhang S, Zahed MA, Sharifuzzaman M, Yoon S, Hui X, et al. 2021. A wearable battery-free wireless and skin-interfaced microfluidics integrated electrochemical sensing patch for on-site biomarkers monitoring in human perspiration. *Biosens. Bioelectron.* 175:112844
82. Choi J, Xue Y, Xia W, Ray TR, Reeder JT, et al. 2017. Soft, skin-mounted microfluidic systems for measuring secretory fluidic pressures generated at the surface of the skin by eccrine sweat glands. *Lab Chip* 17:2572–80
83. Choi J, Kang D, Han S, Kim SB, Rogers JA. 2017. Thin, soft, skin-mounted microfluidic networks with capillary bursting valves for chrono-sampling of sweat. *Adv. Healthc. Mater.* 6:1601355
84. Choi J, Bandodkar AJ, Reeder JT, Ray TR, Turnquist A, et al. 2019. Soft, skin-integrated multifunctional microfluidic systems for accurate colorimetric analysis of sweat biomarkers and temperature. *ACS Sens.* 4:379–88
85. Anastasova S, Crewther B, Bembnowicz P, Curto V, Ip HMD, et al. 2017. A wearable multisensing patch for continuous sweat monitoring. *Biosens. Bioelectron.* 93:139–45
86. Reeder JT, Choi J, Xue Y, Gutruf P, Hanson J, et al. 2019. Waterproof, electronics-enabled, epidermal microfluidic devices for sweat collection, biomarker analysis, and thermography in aquatic settings. *Sci. Adv.* 5:eaau6356
87. Xiao J, Liu Y, Su L, Zhao D, Zhao L, Zhang X. 2019. Microfluidic chip-based wearable colorimetric sensor for simple and facile detection of sweat glucose. *Anal. Chem.* 91:14803–7

88. Mach AJ, Adeyiga OB, Di Carlo D. 2013. Microfluidic sample preparation for diagnostic cytopathology. *Lab Chip* 13:1011–26
89. Zhao J, Guo H, Li J, Bandodkar AJ, Rogers JA. 2019. Body-interfaced chemical sensors for noninvasive monitoring and analysis of biofluids. *Trends Chem.* 1:559–71
90. Sotoudegan MS, Mohd O, Ligler FS, Walker GM. 2019. Paper-based passive pumps to generate controllable whole blood flow through microfluidic devices. *Lab Chip* 19:3787–95
91. Yang Y, Xing S, Fang Z, Li R, Koo H, Pan T. 2017. Wearable microfluidics: fabric-based digital droplet flowmetry for perspiration analysis. *Lab Chip* 17:926–35
92. Ghaffari R, Choi J, Raj MS, Chen S, Lee SP, et al. 2020. Soft wearable systems for colorimetric and electrochemical analysis of biofluids. *Adv. Funct. Mater.* 30:1907269
93. Benito-Lopez F, Coyle S, Byrne R, Smeaton A, O'Connor NE, Diamond D. 2009. Pump less wearable microfluidic device for real time pH sweat monitoring. *Proc. Chem.* 1:1103–6
94. Gao Y, Hou M, Yang R, Zhang L, Xu Z, et al. 2019. Highly porous silk fibroin scaffold packed in PEGDA/sucrose microneedles for controllable transdermal drug delivery. *Biomacromolecules* 20:1334–45
95. Jiang H, Woodhouse I, Selvamani V, Ma JL, Tang R, et al. 2021. A wireless implantable passive intra-abdominal pressure sensing scheme via ultrasonic imaging of a microfluidic device. *IEEE Trans. Biomed. Eng.* 68:747–58